Proc. Natl. Acad. Sci. USA
Vol. 88, pp. 6750–6754, August 1991
Biophysics

Biological transport processes and space dimension

(reaction-diffusion processes/protein internal motions/conformational fluctuations/ligand migration/ion channel fluctuations)

W. NADLER† AND D. L. STEIN‡

†Institut für Theoretische Chemie, Universität Tübingen, Auf der Morgenstelle 8, D-7400 Tübingen, Federal Republic of Germany; and ‡Department of Physics, University of Arizona, Tucson, AZ 85721

Communicated by David Arnett, April 11, 1991 (received for review March 7, 1991)

ABSTRACT **We discuss the generic time behavior of reaction-diffusion processes capable of modeling various types of biological transport processes, such as ligand migration in proteins and gating fluctuations in ion channel proteins. The main observable in these two cases, the fraction of unbound ligands and the probability of finding the channel in the closed state, respectively, exhibits an algebraic $t^{-1/2}$ decay at intermediate times, followed by an exponential cutoff. We provide a simple framework for understanding these observations and explain their ubiquity by showing that these qualitative results are *independent* of space dimension. We also derive an experimental criterion to distinguish between a one-dimensional process and one whose effective dimension is higher.**

Transport processes in biological systems can often be described as reaction-diffusion processes either in real space or in a configuration space of some appropriate dimension. A prominent example of the former is the diffusive transport of biological molecules through the cell protoplasm from the site where they are produced or incorporated to the location where they are needed and absorbed. Adam and Delbrück (1) pointed out the importance of dimensionality in such processes, by observing that an effective reduction of the dimension of the diffusion space—e.g., by restricting the motion of those molecules to certain network structures that pervade the cell—can be utilized to speed up this transport.

In this paper we will be concerned with a different question: How does the time behavior of such transport processes depend on the space dimension involved, and, consequently, can experimental observation give any information on it? Our attention was drawn to this problem while investigating ligand migration through protein matter. Consider, for example, the most thoroughly researched case: ligand migration through myoglobin (Mb) (2–9). Because no channel of sufficient size is available in the averaged static conformation of the protein (10), diffusion of ligand molecules (CO or O_2) through the protein matrix cannot occur in the absence of conformational fluctuations (4, 11, 12). The question then arises whether the ligand motion through the protein matrix is effectively three-dimensional or whether the necessary protein fluctuations occur only within a lower-dimensional subspace (the *single-channel hypothesis*) (4, 13).

Usually, the ligand diffusion process can be experimentally studied only indirectly: bound ligands are separated from the active site by flash photolysis and the fraction of unbound ligands after a time t is monitored (2). The nonexponential rebinding kinetics then observed at low temperatures (process I, below 170 K) is commonly ascribed to a distribution of reaction barriers (2). At higher temperatures the ligand wanders off into the protein matrix (processes II and higher), and this diffusion process is also reflected in the rebinding curve. The time dependence of the curve that results from this diffusion is typically seen to exhibit a $t^{-1/2}$ behavior within a certain range of temperatures and time scales, crossing over to an exponential at longer times (2, 4, 5). This behavior is often taken as evidence that the diffusion regime is effectively a one-dimensional process; however, we will show that this conclusion is incorrect. In fact, the $t^{-1/2}$ falloff is rather ubiquitous and is also seen in other situations, most notably in the integrated closing time distribution of fluctuations in ion channel proteins. It is therefore of interest not only to find a simple yet realistic model to account for this behavior but also to explain its appearance in widely varying situations; we try to answer both of these questions in this paper.

In the following we will analyze processes II and higher of the above sketched experimental situation in terms of a free diffusion process of a ligand in d dimensions subject to a reactive boundary condition (corresponding in the Mb case to rebinding at the surface of the heme pocket). By not specifying the dimension in advance we allow for the possibility that the effective dimension of the diffusion space accessible to the ligand is lower than the dimension of the embedding space (which is three, obviously), leaving open the possibility of channels (corresponding to $d = 1$).

By discussing the diffusion process in general dimensions we also leave open the possibility of applying our model to other biophysical situations that involve diffusion in a much higher-dimensional configuration space ($d >> 3$). For example, fluctuations between protein states of different functionality can be described on a more microscopic level as a stochastic motion through the configuration space of the protein, different regions of which correspond to different macrostates. The open-state/closed-state fluctuations of ion channel proteins are a prominent candidate for such an approach (14). We will see that our model can also be employed to answer questions concerning this problem.

LIGAND MIGRATION

Model. We will describe the migration of a ligand through protein matter in globular proteins as a free diffusion process in d dimensions—i.e., the protein matrix is assumed, for simplicity, to be homogeneous and isotropic. Although this assumption might seem at first to be wholly inappropriate for proteins, the results of our paper are completely unaffected by it. Even the most extreme anisotropies, which are equivalent to reducing the effective dimension of transport, do not affect the behavior of interest because our conclusions will turn out to be independent of dimension.

The diffusion equation for the radial probability distribution $p(r, t)$ of the ligand is then

$$\frac{\partial}{\partial t} p(r, t) = D\left[\frac{\partial^2}{\partial r^2} + \frac{d-1}{r}\frac{\partial}{\partial r}\right] p(r, t). \qquad [1]$$

We note that the diffusion coefficient D in Eq. 1 is considered to be renormalized with respect to local channel/free volume fluctuations within the protein matrix. Since the motion of a

The publication costs of this article were defrayed in part by page charge payment. This article must therefore be hereby marked "*advertisement*" in accordance with 18 U.S.C. §1734 solely to indicate this fact.

ligand through the dense protein matrix has to be facilitated by protein internal fluctuations, the motion of the ligand is coupled to the opening and closing of local channels and/or the creation of local free volumes. However, these processes result mainly in a renormalization of the effective diffusion coefficient D (this will be shown in a future paper). The value of D will depend on the interplay between the time scale of measurement and the rate of physically relevant fluctuations and, therefore, on temperature, pressure, and other environmental parameters experienced by the protein. Though important for a complete theory, these dependences do not affect the conclusions presented here.

For simplicity we will only treat a reflective boundary at some radius R_1 (which is about the radius of the protein):

$$j(r, t)|_{r=R_1} = 0, \quad [2]$$

$j(r, t)$ being the radial probability current,

$$j(r, t) = -D\frac{\partial}{\partial r} p(r, t). \quad [3]$$

Eq. 2 corresponds to zero net flux across the outer boundary, which can describe two different physical situations—either the ligand cannot escape into the solvent surrounding the protein or the outflux from the protein equals the influx of ligands from the solvent. Both situations can be realized experimentally (2). We emphasize that the main results we will present here apply also to situations in which the net flux across the outer boundary is nonzero.

The inner boundary condition arises from the ligand binding process, which takes place at the active site within the protein. We model this binding through a reactive boundary condition at an inner shell with radius R_0 (in Mb, of the order of the size of the heme cavity):

$$j(r, t)|_{r=R_0} = -\gamma p(R_0, t), \quad [4]$$

where the reaction coefficient γ governs the rate at which rebinding takes place at the active site—i.e., ligands are absorbed with a specified rate upon arrival at R_0.

The reactive boundary condition Eq. 4 can be extended readily to more general situations, including nonexponential rebinding arising from (*i*) proteins frozen into conformational substates, giving rise to a distribution, $g(\gamma)$, of rate coefficients γ, or (*ii*) the rebinding process being dynamically coupled to other degrees of freedom, giving rise to a fluctuating rate coefficient $\gamma(t)$. These complications, however, are unlikely to play a significant role at temperatures and time scales in which diffusion of the ligand through the protein matrix makes an important contribution to the observed rebinding curve, and we therefore confine our attention to Eq. 4.

To compare our model with, for example, flash photolysis experiments in Mb, we use the initial condition that the ligand enters the diffusion volume at R_0—i.e.,

$$p(r, t = 0) = \delta(r - R_0)/r^{d-1}. \quad [5]$$

There it can either rebind with a rate γ to the active site or diffuse into the protein matrix and be rebound later.

Introducing the reactive length and time scales $l_r = D/\gamma$ and $\tau_r = D/\gamma^2$, we solve Eq. 1 by means of a spectral expansion

$$p(r, t) = \sum_n \exp(-k_n^2 t/\tau_r)\psi_n(r)\psi_n(R_0), \quad [6]$$

which for general d can be expressed in terms of Bessel functions. The eigenfunctions are

$$\psi_n(r) = (r/l_r)^{1-d/2}\,[a_n J_{1-d/2}(k_n r/l_r) + b_n Y_{1-d/2}(k_n r/l_r)], \quad [7]$$

where J and Y are the (linearly independent) Bessel functions of the first and second kind, respectively (15). In one dimension the eigenfunctions simplify to sine and cosine functions. The eigenvalues k_n and the amplitudes a_n and b_n can now be determined using a standard calculation, which involves using the boundary conditions (Eqs. 2 and 4) to arrive at nonlinear equations for k_n, a_n, and b_n. We omit further details here; a full treatment will be presented in a longer paper.

Results. The reaction-diffusion model as described above exhibits a generic behavior whose gross features are independent of dimension. A typical curve is shown for a particular $3d$ case in Fig. 1: After a fast initial transient within a time of the order of τ_r the unreacted fraction of ligands, $N(t)$, given by

$$N(t) = \int_{R_0}^{R_1} p(r, t) r^{d-1} dr, \quad [8]$$

shows a $t^{-1/2}$ decay, *independent* of the underlying space dimension d. During this algebraic decay the ligand distribution equilibrates in the diffusion volume (or at least in a layer around the reactive boundary), giving rise (in a log–log plot) to a plateau in $N(t)$ after a crossover time τ^*. This quasi-equilibrated state finally decays exponentially with a time constant $\tau_l >> \tau^*$. We note, as will be discussed in more detail below, that some parts of the behavior described above may be absent depending on the particular values of the parameters d, $\Delta R = (R_1 - R_0)/l_r$, and $X = \Delta R/R_0$.

The dimension independence of the transient short-time behavior and of the algebraic decay can be proved by analytical means; such a proof will be presented in a longer paper. We hereafter confine ourselves to a discussion of analytical and numerical results mainly in one and three dimensions, which are clearly the dimensions of interest for the ligand diffusion problem.

The initial two regimes can be understood more easily by considering the $1d$ case without a reflecting boundary, which can be treated analytically (unpublished results). In that case the solution for $N(t)$ is:

$$N_{1d}(t) = \exp(t/\tau_r)\mathrm{erfc}(\sqrt{t/\tau_r}), \quad [9]$$

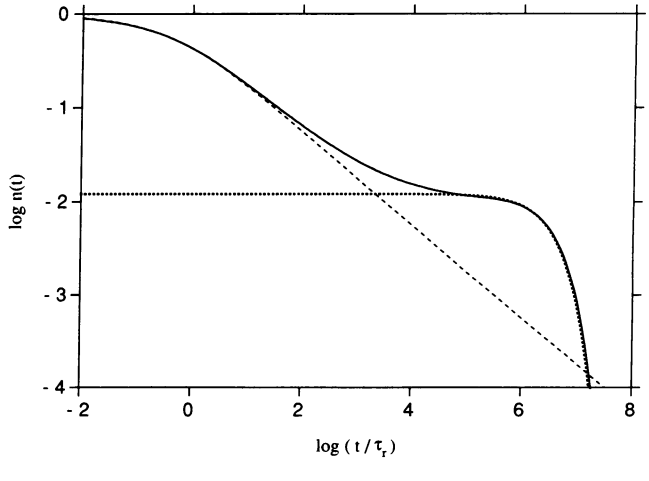

FIG. 1. Generic behavior of the fraction of unbound ligands, $N(t)$. The solid line represents the numerical solution to Eqs. 1–4 by means of the eigenfunction expansion described in the text, with $d = 3$, $\Delta R = 10^3$, and $X = 10$; the dashed line corresponds to Eq. 9, and the dotted line corresponds to Eq. 11.

[erfc is the complementary error function (15)], which is also shown in Figs. 1–3, for comparison. It clearly exhibits the asymptotic algebraic $t^{-1/2}$ decay after a transient time of order τ_r:

$$\lim_{t\to\infty} N_{1d}(t) \to \sqrt{\frac{1}{\pi t/\tau_r}} + O(t^{-3/2}). \qquad [10]$$

Without any boundary at R_1 the algebraic decay (10) would go on indefinitely in one dimension. However, the reflecting boundary at R_1, a finite size effect, introduces an exponential cutoff for the long-time behavior. The effect of this cutoff in one dimension is shown in Fig. 2 for different values of ΔR. This single-exponential cutoff can be described by

$$\lim_{t\to\infty} N(t) \approx q_l e^{-t/\tau_l}. \qquad [11]$$

It can be seen clearly that the larger the value of ΔR, the larger the cutoff time τ_l and the smaller the corresponding amplitude q_l. The $t^{-1/2}$ regime is only present when $\tau_l >> \tau_r$. For small values of ΔR—i.e., when τ_l and τ_r have the same order of magnitude—the $t^{-1/2}$ regime vanishes altogether.

Fig. 3 shows the behavior of $N(t)$ in three dimensions. In addition to the regimes present in the $1d$ case, one can see the emergence, for large values of X, of the plateau regime between the algebraic regime and the exponential cutoff in the log–log plot. This plateau regime is due to an equilibration of the ligand distribution within the protein matrix: a majority of the ligands accumulate far from the reactive boundary, and their number decays exponentially with a time constant τ_l. Such an accumulation is possible only when the diffusion space is large, with the bulk of it far from the reactive boundary. In particular, this condition is fulfilled only when $d > 1$ and for sufficiently large values of the parameter X.

The amplitude q_l and the time scale τ_l of the single-exponential cutoff, Eq. **11**, can be determined by an approximation using the generalized moments (16) of the unreacted fraction $N(t)$:

$$\mu_{-n} = (n-1)! \int_0^\infty t^{n-1} N(t) dt. \qquad [12]$$

In this particular case a long-time approximation is appropriate (16), giving $\tau_l = \mu_{-2}/\mu_{-1}$ and $q_l = \mu_{-1}^2/\mu_{-2}$. Those moments can be determined analytically for the problem governed by Eqs. **1–4** (16–18), with the result

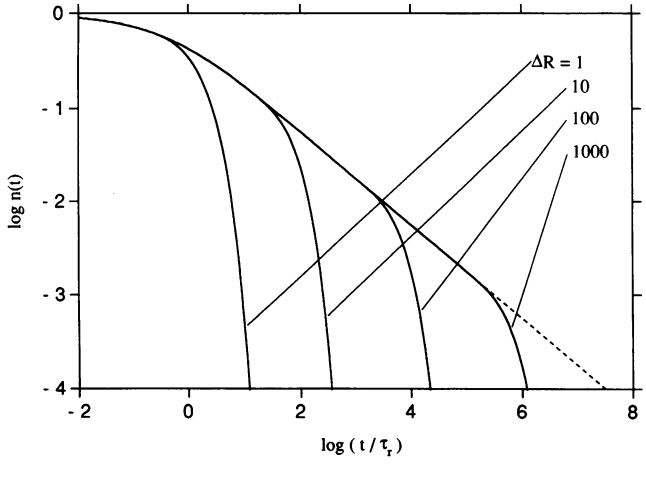

FIG. 2. Fraction of unbound ligands, $N(t)$, in *one* dimension; parameter ΔR = 1, 10, 100, and 1000 (from left to right); the dashed line corresponds to Eq. **9**.

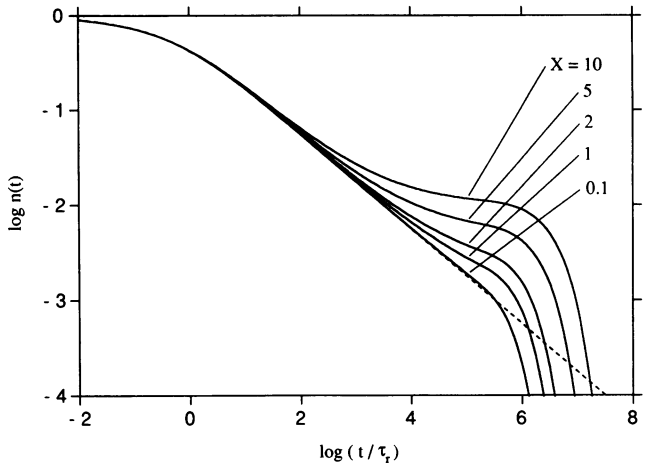

FIG. 3. Fraction of unbound ligands, $N(t)$, in *three* dimensions; $\Delta R = 10^3$ and X = 10, 5, 2, 1, and 0.1 (from top to bottom); the dashed line corresponds to Eq. **9**.

$$\mu_{-1} = \tau_r \Delta R (Y^d - 1)/Xd \qquad [13a]$$

$$\mu_{-2} = \{\tau_r^2/X^3 d^2 (d^2-4)\} \times \{\Delta R^2 X (Y^d-1)^2 (d^2-\ ) + \Delta R^3 [2 - d + Y^d(d^2-4) - Y^{2+d} d^2 + Y^{2d}(d+2)]\}, \qquad [13b]$$

where $Y = (1 + X)$.

These results on the exponential long-time cutoff allow us to analyze the algebraic regime and the plateau regime more quantitatively. One necessary condition for the algebraic regime to be present is that the cutoff time scale τ_l is much larger than the time for the initial transient, τ_r. This condition is controlled by the dimensionless function

$$g(\Delta R, X, d) \equiv \frac{\tau_l}{\tau_r} = \frac{\mu_{-2}}{\tau_r \mu_{-1}}. \qquad [14]$$

A crossover time τ^* from the algebraic $t^{-1/2}$ decay to the plateau regime can be estimated through the relation

$$N_{1d}(\tau^*) \approx q_l, \qquad [15]$$

giving rise to

$$\tau^* \approx \tau_r/\pi q_l^2. \qquad [16]$$

The other condition for the existence of the algebraic regime is that this crossover time τ^* is also much larger than the initial transient time τ_r. The dimensionless function

$$h(\Delta R, X, d) \equiv \frac{\tau^*}{\tau_r} = \frac{1}{\pi}\frac{\mu_{-2}^2}{\mu_{-1}^4} \qquad [17]$$

controls this second condition. For the algebraic regime to be present, both functions g and h have to be much larger than unity. In one dimension, we find $g = \Delta R(1 + \Delta R/3)$ and $h = \frac{1}{\pi}(1 + \Delta R/3)^2$. In dimensions $d > 1$, ΔR fixed, and $X \to \infty$, we find $g \propto X^{d-1}$, while $h \to \pi^{-1}$; for dimensions $d > 1$, X fixed, and $\Delta R \to \infty$, both functions scale as ΔR^2. From these results it can be seen that for given values of X and d, the conditions $g >> 1$ and $h >> 1$ can both be met, provided ΔR is large enough. This supports the conclusions we drew from Figs. 2 and 3. Since h decreases as X increases, large values of X can shorten the algebraic regime, and, in the limit of

$X \to \infty$, let it vanish altogether. This shortening of the algebraic regime can also be seen in Fig. 3.

The plateau regime will be clearly visible only for $\tau_l >> \tau^*$; otherwise, the algebraic regime will cross over directly to the exponential tail. Therefore, the function

$$f(\Delta R, X, d) \equiv \frac{\tau_l}{\tau^*} = \frac{g}{h} \quad [18]$$

controls the existence of the plateau regime. This function grows monotonically with ΔR, X, and d, and its asymptotic properties follow directly from the asymptotic properties of g and h discussed above. In $1d$, we find $f \to 3\pi$ in the limit $\Delta R \to \infty$; the condition $f >> 1$ for having a plateau is just barely fulfilled. However, because q_l vanishes in the limit $\Delta R \to \infty$ the plateau will not, in fact, be visible. The difference in the present situation between one and higher dimensions is that for $d > 1$ the function f becomes infinite for $X \to \infty$ (even for finite ΔR), whereas in one dimension f always remains small. We conclude, therefore, that a plateau regime will be seen in dimensions two and higher, provided that the values of X and ΔR are large enough. This conclusion is also supported by numerical results (unpublished results). Note that the parameter X, which describes the ratio of the thickness of the d-dimensional shell to its inner radius of curvature, controls the effective dimensionality of the diffusion shell. $X \to 0$ is the limit of an extremely thin diffusion shell and corresponds, therefore, to a $1d$ situation, whereas $X \to \infty$ corresponds to a d-dimensional sphere of radius R_1 with an absorptive point in the center.

Discussion. There are several important conclusions to be drawn from the results presented above. We first address a common misconception about the $N(t) \propto t^{-1/2}$ behavior. The usual approach is to assume a free one-dimensional diffusion process, starting at R_0. Because ligands are assumed to disappear upon returning to R_0, one clearly needs to evaluate $p(R_0, t)$, the probability of return at time t to the starting point R_0. For free diffusion $p(R_0, t) \to t^{-d/2}$ as $t \to \infty$ in d dimensions. By identifying this with the $N(t) \propto t^{-1/2}$ behavior, one is tempted to conclude $d = 1$. This is, however, not correct, because the measured quantity $N(t)$ (the unreacted fraction of ligands) and the theoretical quantity $p(R_0, t)$ do *not* have the same time dependence. It is easy to show, using Eq. **8** together with Eqs. **1–4**, that $(d/dt)N(t) = -\gamma p(R_0, t)$, which would lead to $N(t) \propto t^{-(d-2)/2}$, and a $t^{-1/2}$ behavior would be consistent only with three dimensions. In any case, it is important to note that a model with an absorbing or reacting boundary at R_0 exhibits a behavior *different* from the free diffusion case.

This leads us to our main conclusions:

(*i*) The appearance of a $t^{-1/2}$ regime for the unreacted fraction $N(t)$ is a reaction-diffusion process described in Eqs. **1–4** is quite robust and independent of the space dimensionality of the process. It should be expected—for large enough values of ΔR and X not too large—whenever there exists a diffusion region of shell-like structure controlled by a reactive boundary condition.

We remark here briefly about this dimension independence. For an absorbing inner boundary and *no* outer boundary, $N(t)$ in both one and three dimensions shows $t^{-1/2}$ decay (although in $3d$ the decay does not extend to zero). In other dimensions, and in the geometry discussed in the preceding paragraph, absorption of the boundary layer (effectively a $1d$ situation) dominates the algebraic part of the overall decay of $N(t)$. Numerical support and an analytical proof of these statements, along with a more extensive discussion, will be presented in a longer paper.

(*ii*) By the same token, the existence of an algebraic $t^{-1/2}$ regime in the decay of the ligand fraction $N(t)$ in ligand migration and rebinding experiments is by no means conclusive evidence for a $1d$ process taking place. On the contrary, such an algebraic decay is highly unspecific with regard to the space dimensionality of the process: for a wide parameter range it will be observed also in higher-dimensional systems. Nevertheless, the time scale of that algebraic regime, τ_r, gives important information concerning the ratio of the diffusion coefficient to the binding rate.

(*iii*) However, there is a clear experimental signature that differentiates between one-dimensional diffusion and an effectively higher-dimensional process: our results demonstrate that the observation of a plateau in a log–log plot of $N(t)$ vs. t following the algebraic decay regime indicates that the diffusion path of the ligand is effectively higher-dimensional. Its existence is controlled mainly by the effective dimensionality of the diffusion shell—i.e., the parameters d and X. We note that plateau-like regimes in $N(t)$ have already been observed but have been attributed partly to escape into the solvent [processes III and IV of Austin *et al.* (2)]. Our results indicate that these regimes could also be a signature of the three-dimensionality of the ligand migration process.

(*iv*) The exponential cutoff of the rebinding curve, which previously had not been treated thoroughly, is now also accessible to analysis by employing the above results.

ION CHANNEL FLUCTUATIONS

Open-state/closed-state fluctuations of ion channel proteins can be modeled on a more microscopic, although also more abstract, level as a random motion of the protein in its configuration space, different patches of which correspond to either one of the two different macrostates, respectively. In this approach, a channel that switches, for example, from the open to the closed state can be thought of as crossing the boundary from a region of open-state configurations to a region of closed-state configurations. There are three relevant topologies for the respective structures of open- and closed-state regions in the d-dimensional configuration space—either both percolate throughout the entire space or one percolates but not the other (having neither percolate requires special geometries and is unlikely to be encountered). It is not known which of these actually applies to the ion channel problem. Our model can clearly be applied when patches of open states are completely surrounded by closed states (and also in other circumstances to be discussed in a future paper). Most important, the interface between open and closed states must be $(d - 1)$-dimensional. Diffusion occurs in the closed state region until the system leaves this region by crossing the boundary into the open state region. The reactive boundary condition then naturally corresponds to the crossing of the boundary from the closed to the open region; upon encountering the boundary, either the system continues to wander into the open state region (absorption) or it immediately returns into the closed state region. The parameter γ is connected with the relative frequency of these two events. The conditional probability of observing a channel in the closed state at time t, given that it switched to the closed state at $t = 0$, then corresponds to the quantity $N(t)$, and the closed-state time distribution is given by $(-d/dt)N(t)$.

A number of recent studies (19–27) undertake to explain the $t^{-3/2}$ closed-state time distribution observed in many ion channel proteins through models featuring specific realizations of the above discussed configuration space partitioning. In those studies mainly one-dimensional descriptions were considered [the microscopic defect diffusion model of Läuger (19) and the percolation model of Doster *et al.* (14) are notable exceptions]. In many of these models a discrete configuration space was employed; although such an approach may give results different from our continuous model if a small number of states are involved, the results will be qualitatively equiv-

alent for a large number of states (incidentally, the latter case is just the limit for which the $t^{-3/2}$ distribution is obtained in those models).

In light of our above results—i.e., the $N(t) \propto t^{-1/2}$ behavior for most parameter regimes—it is no surprise that those one-dimensional models could reproduce the $t^{-3/2}$ closed-time distribution. Any description that models the patch of closed states in configuration space as a one-dimensional interval will show such a behavior.

However, our result for general dimensions raises the caveat that one should not take the actual one-dimensionality of any of these models too literally. Higher-dimensional model descriptions would arrive at the same closed-time distribution for a wide range of parameter values. The particular properties of the actual protein configuration space will be reflected only in *deviations* from the algebraic behavior, as in the previously discussed plateau regime.

Note Added in Proof. As this paper went to press, we learned of recent related work (28). We thank Peter Wolynes for bringing this to our attention.

W.N. thanks the Physics Department and the Center for the Study of Complex Systems at the University of Arizona for generously supporting extended visits during which much of this work was done. Stimulating discussions with W. Doster and M. Aizenman are gratefully acknowledged.

1. Adam, G. & Delbrück, M. (1968) in *Structural Chemistry and Molecular Biology*, eds. Rich, A. & Davidson, N. (Freeman, San Francisco), pp. 198–215.
2. Austin, R. H., Beeson, K. W., Eisenstein, L., Frauenfelder, H. & Gunsalus, I. C. (1975) *Biochemistry* **14**, 5355–5373.
3. Alberding, N., Chan, S. S., Eisenstein, L., Frauenfelder, H., Good, D., Gunsalus, I. C., Nordlund, T. J., Perutz, M. F., Reynolds, A. H. & Sorensen, L. B. (1978) *Biochemistry* **17**, 43–51.
4. Beece, D., Eisenstein, L., Frauenfelder, H., Good, D., Marden, M. C., Reinisch, L., Reynolds, A. H., Sorensen, L. B. & Yue, K. T. (1980) *Biochemistry* **19**, 5147–5157.
5. Doster, W., Beece, D., Bowne, S. F., Di Iorio, E. E., Eisenstein, L., Frauenfelder, H., Reinisch, L., Shyamsunder, E., Winterhalter, K. H. & Yue, K. T. (1982) *Biochemistry* **21**, 4831–4839.
6. Ansari, A., Berendzen, J., Bowne, S. F., Frauenfelder, H., Iben, I. E. T., Sauke, T. B., Shyamsunder, E. & Young, R. D. (1985) *Proc. Natl. Acad. Sci. USA* **82**, 5000–5004.
7. Ansari, A., Di Iorio, E., Dlott, D., Frauenfelder, H., Iben, I. E. T., Langer, P., Roder, H., Sauke, T. B. & Shyamsunder, E. (1986) *Biochemistry* **25**, 3139–3146.
8. Ansari, A., Berendzen, J., Braunstein, D., Cowen, B. R., Frauenfelder, H., Hong, M. K., Iben, I. E. T., Johnson, J. B., Ormos, P., Sauke, T. B., Scholl, R., Schulte, A., Steinbach, P. J., Vittitow, J. & Young, R. D. (1987) *Biophys. Chem.* **26**, 337–355.
9. Frauenfelder, H., Alberding, N. A., Ansari, A., Braunstein, D., Cowen, B. R., Hong, M. K., Icko, E., Johnson, B. J., Luck, S., Marden, M. C., Mourant, J. R., Ormos, P., Reinisch, L., Scholl, R., Schulte, A., Shyamsunder, E., Sorensen, L. B., Steinbach, P. J., Xie, A., Young, R. D. & Yue, K. T. (1990) *J. Phys. Chem.* **94**, 1024–1037.
10. Case, D. A. & Karplus, M. (1979) *J. Mol. Biol.* **132**, 343–368.
11. Karplus, M. & McCammon, J. A. (1981) *CRC Crit. Rev. Biochem.* **9**, 293–349.
12. Stein, D. L., Palmer, R. G., van Hemmen, J. L. & Doering, C. (1989) *Phys. Lett. A* **136**, 353–357.
13. Hänggi, P. (1983) *J. Stat. Phys.* **30**, 401–412.
14. Doster, W., Schirmacher, W. & Settles, M. (1990) *Biophys. J.* **57**, 681–684.
15. Abramowitz, M. & Stegun, I. A. (1972) *Handbook of Mathematical Functions* (Dover, New York).
16. Nadler, W. & Schulten, K. (1985) *J. Chem. Phys.* **82**, 151–160.
17. Szabo, A., Schulten, K. & Schulten, Z. (1980) *J. Chem. Phys.* **72**, 4350–4357.
18. Schulten, K., Schulten, Z. & Szabo, A. (1981) *J. Chem. Phys.* **74**, 4426–4432.
19. Läuger, P. (1988) *Biophys. J.* **53**, 877–884.
20. Korn, S. J. & Horn, R. (1988) *Biophys. J.* **54**, 871–877.
21. McManus, O. B., Weiss, D. S., Spivak, C. E., Blatz, A. L. & Magleby, K. L. (1988) *Biophys. J.* **54**, 859–870.
22. Millhauser, G. L. & Oswald, R. E. (1988) *Synapse (NY)* **2**, 97–107.
23. Millhauser, G. L., Salpeter, E. E. & Oswald, R. E. (1988) *Biophys. J.* **54**, 1165–1168.
24. Millhauser, G. L., Salpeter, E. E. & Oswald, R. E. (1988) *Proc. Natl. Acad. Sci. USA* **85**, 1503–1507.
25. Millhauser, G. L. (1990) *Biophys. J.* **57**, 857–864.
26. Condat, C. A. (1989) *Phys. Rev. A* **39**, 2112–2125.
27. Condat, C. A. & Jäckle, J. (1989) *Biophys. J.* **55**, 915–925.
28. Miers, J. B., Postlewaite, J. C., Zyung, T., Chen, S., Roomig, G. R., Won, X., Dlott, D. D. & Szabo, A. (1990) *J. Chem. Phys.* **93**, 8771–8776.